CONFIDENTIAL

Copy 5
RM L53I25b

NACA RM L53I25b

NACA

RESEARCH MEMORANDUM

SOME CONSIDERATIONS CONCERNING INLETS AND DUCTED BODIES AT MACH NUMBERS FROM 0.8 TO 2.0

By Richard I. Sears

Langley Aeronautical Laboratory
Langley Field, Va.

CLASSIFIED DOCUMENT

NATIONAL ADVISORY COMMITTEE
FOR AERONAUTICS

WASHINGTON

November 24, 1953

CONFIDENTIAL

[redacted]

NATIONAL ADVISORY COMMITTEE FOR AERONAUTICS

RESEARCH MEMORANDUM

SOME CONSIDERATIONS CONCERNING INLETS AND DUCTED BODIES AT MACH NUMBERS FROM 0.8 TO 2.0

By Richard I. Sears

SUMMARY

Some of the large differences that can exist at supersonic speeds in the pressure recovery and drag of good and not-so-good inlet and engine installation arrangements are pointed out. Best pressure-recovery results have been obtained with scoop inlets located close under the nose and, for farther rearward locations, with external compression inlets having complete boundary-layer removal. Best drag results have been obtained with conical nose inlets, with scoop inlets located close to the nose and causing little or no increase in frontal area, and with a wing-root-inlet buried-engine configuration.

INTRODUCTION

The study of air-inlet design is essentially a study of thrust and drag. With an adequately sized inlet, the thrust available is proportional to the total pressure the inlet can provide. Many data have been presented in the past concerning the pressure recoveries attainable at supersonic Mach numbers with various types of inlets. Some information on this subject is presented in this paper.

Much less data relative to the drag of bodies having air inlets and internal-flow systems are available. The drag characteristics of nonducted bodies of revolution as affected by various shape parameters have been fairly well established and a considerable amount of experimental data is published. Incorporation in a body of a turbojet engine and its associated inlets and ducting can cause a major departure in geometry from the more idealized body of revolution.

This paper presents some drag information from systematic tests of nose inlets and from isolated tests of scoop and wing root inlets.

[redacted]

SYMBOLS

A	area
C_D	drag coefficient, based on fuselage frontal area
$\left(C_{D_o}\right)_W$	zero-lift drag coefficient, based on wing exposed area
$\frac{m}{m_o}$	mass-flow ratio
$\frac{\bar{H}}{H_o}$	average total-pressure-recovery ratio
α	angle of attack
M	Mach number
θ_l	cone position angle (see fig. 3)
δ_l	cowl lip angle (see fig. 3)

Subscripts:

i	inlet (taken at lip leading edge)
f	fuselage frontal
o	free stream

DISCUSSION

Nose inlets.- Figure 1 shows configurations tested by means of rocket techniques to evaluate effects of cowling profile on the drag of normal-shock nose inlets. Five different cowl shapes were tested, each with identical afterbody shape, and are shown in figure 1. All cowls were of fineness ratio 3 and the inlet area was 24 percent of the body frontal area. Over-all model fineness ratio was 8. The top cowl is of the NACA 1-series family; the second is defined by a parabolic arc with its vertex at the maximum diameter. The next three are conical with beveled, blunt, and sharp lips, respectively.

[redacted]

Figure 2 shows the measured external drag coefficient C_D (based on body frontal area) of the complete models, at the left as a function of M for $\frac{m}{m_o} = 1$, and at the right as a function of m/m_o for $M = 1.3$. For maximum flow rate at Mach numbers up to about 1.1, all cowl shapes have about the same C_D, but the curves spread apart at higher M, the 1-series cowl having the greatest C_D and the cone with sharp lips the least. The other cowls fell in between and in the same order as shown in figure 1. The solid line gives the drag of the nonducted, pointed body, derived by extending the lines of the parabolic cowling as shown at the top of figure 1. The drag of the models with conical cowls are significantly lower than that of the pointed body because of the air admitted.

At $M > 1.35$, the value of C_D for the body with blunt-lip conical cowl is about 0.04 less than that for the 1-series cowl. Since both the 1-series cowl and the blunt-lip conical cowl had identical profiles in the region of the inlet lip, it is apparent that the lower drag of this conical cowl is associated with its lesser fullness of profile farther back than the region of the lips.

The curves of figure 2 show that at $M = 1.3$ all cowls except the 1-series have about the same value of C_D at $\frac{m}{m_o} \approx 0.8$. Thus, whereas the sharp-lip configuration had least drag at maximum flow rate, the beveled and blunt-lip conical cowls gave less increase in C_D as air was spilled. Actually, the increase in C_D for the sharp-lip conical cowl is just about equal to the additive drag calculated from momentum considerations. The other inlets all benefit to some extent from leading-edge suction, the increment in C_D associated with spilling air being less than the computed additive drag. The fact that blunt lips can be tolerated on conical cowls without large drag penalties is encouraging because they may be necessary structurally and for operation at take-off and at angles of attack.

The effect of cowl shape on the drag of conical-shock nose-inlet models in the transonic and supersonic range has been recently obtained from rocket tests. The configurations tested are shown in figure 3. The models had afterbodies and fins similar to those of figure 1. The cowls were of fineness ratio 3 and the inlet area was 24 percent of the body frontal area. The cowls had external lip angles of 12° and 17° faired into conical and parabolic cowl shapes as shown. The cone position was varied as indicated by the values of θ_l at the right of figure 3.

The data obtained for these models are given in figure 4. The internal flow for each model was the maximum that the inlet would pass

[redacted]

and is given by the upper curves, one for each cone position. The designation for each drag curve specifies first, the cowl shape, parabolic or conical; second, the external lip angle of the cowl; and lastly, the cone position angle.

Inspection of the drag curves shows that changes in lip angle and cone position result in small changes in the drag in the direction to be expected; however, that shown for changes in cone position borders on the accuracy of the tests. The effects of cowl shape are more pronounced. The conical-cowl models had lower drag than did the parabolic-cowl models; this result is consistant with the results shown in figure 2 for the normal-shock nose-inlet models.

The total-pressure recovery at supersonic Mach numbers of nose inlets, with and without external compression, are fairly well known for operation at an angle of attack of 0°. Tests have indicated that at higher angles of attack the pressure recovery decreases rapidly.

Figure 5 shows some results from exploratory tests of a swept inlet expected to have better recovery at high angles of attack than a normal-shock inlet. The latter is also shown for comparison. The swept inlet was made from a circular pipe by cutting it obliquely at 45° to the axis and beveling the lips on the outside. Total-pressure recoveries were measured at $M = 1.42$ without any diffusion and at $M = 1.84$ with some diffusion. The portion of the inlet and duct ahead of the rake station is shown in the sketches. Positive angles of attack are taken as indicated by the arrows. The normal-shock inlet, tested only at $M = 1.42$, had rounded inner lips and some diffusion.

The models were tested with a choking nozzle at the duct exit, which simulates constant-engine-inlet Mach number operation. The mass-flow ratio therefore varied with angle of attack, it being proportional to the pressure recovery. The upper set of curves show the values of mass-flow ratio obtained, and the corresponding pressure recoveries are shown in the lower set of curves.

It appears, from these data, that use of a swept nose inlet provides reasonably good recoveries at positive angles of attack as high as 20° to 30° at the expense of low flow rates and poor recoveries at negative angles of attack. Other published data (ref. 1) show that a swept nose inlet with a vertical-wedge compression surface maintains a nearly constant recovery of about 0.85 for angles of attack from 0° to 10° at $M = 1.9$. The drag characteristics of the swept inlet have not been measured.

Scoop inlets.- Fairly extensive data are available on the pressure recoveries attainable with nose inlets, and these will not be discussed further here. However, in many cases it is not practical to use nose

inlets. Many different types of scoop inlets have been tested with widely differing results dependent, to a large extent, on the treatment of the boundary layer ahead of the inlet.

Figure 6 is intended to give a brief perspective of the relative standing of various types of scoops with regard to total-pressure recovery. The data presented are the maximum average total pressure after diffusion at about an angle of attack of 0° and for mass-flow ratios above 0.75. It is assumed that for a scoop to be considered for use it must have good recovery, at least for these operating conditions. The symbols without flags represent wind-tunnel-data test points and the symbols with flags represent the end points of curves defined by rocket data. The open symbols represent scoops with some type of boundary-layer removal system, whereas the solid points indicate scoops with no boundary-layer removal system. Detailed results for many of these scoops are reported in references 2 to 11. Scoop inlets are of several types as indicated in the lower left corner of figure 6 and by the sketches shown.

The data presented are sample data for each type of scoop, but the maximum recoveries shown are believed quite representative of those that have been obtained for each type. Problems of matching are not considered here.

Inspection of these data indicates that the recoveries obtained at supersonic speeds can be either good or bad depending on the scoop configuration used and on the treatment of the boundary layer. Best recoveries have been obtained with scoops located just under the nose of the body and with external-compression-type scoops having complete boundary-layer removal. At $M < 1.4$ and $m/m_0 > 0.75$, the nose scoop apparently needs no boundary-layer removal and has good recovery at positive angles of attack (refs. 4, 5, and 10). Reference 12 treats the external compression scoop in more detail. Annular or semiannular scoops which enclose an appreciable part of the body circumference give low recoveries and pulsations at reduced flow rates (refs. 2, 3, and 7). The submerged inlet suffers also from boundary-layer shock interaction aggravated by superstream Mach numbers ahead of the inlet, caused by the curving ramp floor inherent in the design (ref. 8).

Whereas the pressure recovery of scoop inlets can be rather easily compared, the drag characteristics cannot be except in special cases where several scoop arrangements are tested for a particular airplane. Such systematic tests are rare. The installation of the power plant, ducting, and scoop inlet largely determine the fuselage lines which, of course, govern the drag. Although drag data for scoop configurations are very meager, it is possible to report the results from several isolated investigations.

[redacted]

Figure 7 shows about all the fuselage models having scoop inlets for which drag data are available. Above the sketch of each configuration, the curve of area distribution normal to the longitudinal axis is shown in order to define the geometry better. The solid line represents areas corresponding to the physical outline of the model and the dashed line represents deduction of the entering free-stream tube area, a procedure which recent tests have shown to result in an equivalent nonducted body having the same drag. All the diagrams are shown to the same scale.

For the upper three models, only the forward portion of the fuselage was tested. Models B, C, and G and the forward half of model E are models of actual aircraft. The models on the left are research configurations.

Drag curves as a function of Mach number are given for some of these configurations in figures 8 and 9 and a comparison of the drag results is given in figure 10. Because these configurations are not related in any manner except that all models had scoop inlets, it is convenient to plot their drag as a function of effective body fineness ratio. This value is taken as the length divided by the diameter of a circle of area equal to the maximum frontal area.

The data are shown at the top of figure 10 for the fuselage nose configurations A, B, and C, and at the bottom of figure 10, for the complete fuselage models. The two solid lines, shown for reference purposes, give the drag of parabolic bodies of revolution without internal air flow. The solid line on the top of figure 10 was computed for parabolic-nose shapes from second-order theory with an allowance for skin friction included. The curve on the bottom of figure 10 was obtained from rocket tests of parabolic bodies of revolution. If the drag shown by these curves at high fineness ratio is taken as that for a good parabolic body of revolution, then the scale at the right gives the ratio of drag to that of a good body.

Many of the models have nearly twice the drag of good bodies and almost all have appreciably more drag than parabolic bodies of the same fineness ratio.

For model E (ref. 7), the area curve shows a forward location for the maximum area station which results in a low nose fineness ratio. Data presented in reference 9 indicated that the increase in drag for model E over that shown in figure 10 by the solid line for a parabolic body of the same over-all fineness ratio and in figure 8 can be just about accounted for on the basis of difference in nose fineness ratio. Thus, although, as shown in reference 12, forwardly located scoops are favorable from boundary-layer considerations, they can cause high drag if they result in a low effective nose fineness ratio.

[redacted]

The forwardly located underslung scoop of model D was added to a parabolic body of revolution without increasing or changing the location of the maximum frontal area. Thus, the nose fineness ratio was not changed and, as indicated by point D on the lower part of figure 10 and by figure 8, the drag of the ducted model was, within the experimental accuracy, the same as that of the body without scoop. Although the scoop of model D had an area only 8 percent of the body frontal area, tests in the Langley 8-foot transonic tunnel (ref. 10) of a similar scoop of area twice as large relative to the fuselage also indicated negligible drag increment, at least to $M = 1.1$, the limit of the test. The underslung nose scoop, therefore, looks good from drag as well as pressure-recovery considerations.

Although the effective fineness ratio (as defined) is fairly large for model C, dragwise it acted like a nose of much lower fineness ratio (ref. 13). The distribution of area in this case was important.

Fuselage drag usually accounts for the greater portion of airplane zero-lift drag. Therefore, it is obviously important to make the drag of fuselages, with scoop inlets and associated bumps for ducting and engine housing, approach the drag of good bodies of revolution. It is recognized that greater research effort is needed to indicate ways of achieving this effect.

Wing root inlet.- Another important class of inlets is the wing root inlet. Data published in reference 14 show that a wing root inlet could be added to an 8-percent-thick swept wing with very little increase in drag at Mach numbers less than 1.4, the limit of the tests. Figure 11 presents data to $M = 2$ which lead to similar conclusions for a somewhat different wing-root-inlet arrangement.

The basic wing was swept 47° on the quarter-chord line and was 5.5 percent thick. Inboard of the one-third semispan station the wing was split and the lower portion dropped to form the root inlet as shown in the sketch. The modified wing root housed two semiburied turbojet engines on each side as well as the inlet. The upper curve gives the mass-flow ratios at which the inlet was operated. The lower two curves give the measured external drag coefficients of the wing. These values are based on exposed-wing plan-form area. The solid points indicate data for the wing with inlet and engine installation and the open symbols are for the unaltered basic wing. These drag coefficients were obtained from tests of the configuration with and without the wing. Wing-fuselage interference drag is thus included in values given in figure 11. The data are given for the zero-lift condition only.

Comparison of the two drag curves indicates that addition of this root inlet increased the wing drag coefficient by about 10 percent at supersonic speeds. Inasmuch as the wing frontal area was increased 20 percent by the inlet, this result means that the drag per unit frontal

[redacted]

area of the wing with inlet and engine installation was only 92 percent of that of the basic wing. This effect is, of course, caused by the fact that the wing was admitting air. However, the reduction in drag per unit frontal area for this wing root inlet and engine configuration is in marked contrast to the increases in drag per unit frontal area shown previously for fuselage configurations having scoop inlets.

Although adequate pressure-recovery data are not available for this inlet configuration, figure 12 shows recoveries measured in the Langley transonic blowdown tunnel for another wing root inlet. Adding this elliptically shaped root inlet to the basic swept wing-fuselage configuration caused increments of drag coefficient of about the same magnitude as those shown in figure 11.

The inlet lips were round and staggered as shown in the sketch. Tests were made with and without a boundary-layer bleed. The basic fuselage lines just ahead of the inlet were altered to permit installation of the boundary-layer bleed scoop. The boundary-layer duct exited normal to the wing on the lower surface just back of the inlet.

The three sets of curves show the effects of Mach number, angle of attack, and mass-flow ratio on the average pressure recovery measured after diffusion, for operation with and without the boundary-layer bleed.

Analysis of the data shown in figure 12 and in figure 11 shows swept-wing root inlets to be potentially low drag configurations and, without external-compression devices, to be potentially capable of giving normal-shock recoveries over a fairly large angle-of-attack range. The need for further development to provide a workable boundary-layer bleed system is indicated.

CONCLUDING REMARKS

This paper has attempted to point out some of the large differences that can exist at supersonic speeds in the pressure recovery and drag of good and not-so-good inlet and engine installation arrangements. Best pressure-recovery results have been obtained with scoop inlets located close under the nose and, for farther rearward locations, with external compression inlets having complete boundary-layer removal. Best drag results have been obtained with conical nose inlets, with scoop inlets located close to the nose and causing little or no increase in frontal area, and with a wing-root-inlet buried-engine configuration. More work is needed to define the minimum-drag arrangements of scoop configurations wherein the engine installation causes large increases in frontal area

[redacted]

of a basically good fuselage. At present, available tests have shown such configurations to be of high drag relative to those previously mentioned.

Langley Aeronauticaly Laboratory,
National Advisory Committee for Aeronautics,
Langley Field, Va., September 9, 1953.

[redacted]

REFERENCES

1. Leissler, L. Abbott, and Hearth, Donald P.: Preliminary Investigation of Effect of Angle of Attack on Pressure Recovery and Stability Characteristics for a Vertical-Wedge-Nose Inlet at Mach Number of 1.90. NACA RM E52E14, 1952.

2. Pendley, Robert E., Milillo, Joseph R., Fleming, Frank F., and Bryan, Carroll R.: An Experimental Study of Five Annular-Air-Inlet Configurations at Subsonic and Transonic Speeds. NACA RM L53F18a, 1953.

3. Davis, Wallace F., Brajnikoff, George B, Goldstein, David L., and Spiegel, Joseph M.: An Experimental Investigation at Supersonic Speeds of Annular Duct Inlets Situated in a Region of Appreciable Boundary Layer. NACA RM A7G15, 1947.

4. Merlet, Charles F., and Carter, Howard S.: Total-Pressure Recovery of a Circular Underslung Inlet With Three Different Nose Shapes at a Mach Number of 1.42. NACA RM L51K05, 1952.

5. Boswinkle, Robert W., Jr., and Mitchell, Meade H., Jr.: Experimental Investigation of Internal-Flow Characteristics of Forward Underslung Fuselage Scoops With Unswept and Sweptback Entrances at Mach Numbers of 1.41 to 1.96. NACA RM L52A24, 1952.

6. Dryer, Murray, and Beke, Andrew: Performance Characteristics of a Normal-Shock Side Inlet Located Downstream of a Canard Control Surface at Mach Numbers of 1.5 and 1.8. NACA RM E52F09, 1952.

7. Carter, Howard S., and Merlet, Charles F.: Flight Determination of the Pressure Recovery and Drag Characteristics of a Twin Side-Inlet Model at Transonic Speeds. NACA RM L53E05, 1953.

8. Braden, John A., and Pierpont, P. Kenneth: Pressure and Force Characteristics at Transonic Speeds of a Submerged Divergent-Walled Air Inlet on a Body of Revolution. NACA RM L53C13, 1953.

9. Nelson, Robert L., and Stoney, William E., Jr.: Pressure Drag of Bodies at Mach Numbers up to 2.0. NACA RM L53I22c, 1953.

10. Pierpont, P. Kenneth, and Braden, John A.: Investigation at Transonic Speeds of a Forward-Located Underslung Air Inlet on a Body of Revolution. NACA RM L52K17, 1953.

11. Wittliff, Charles E., and Byrne, Robert W.: Preliminary Investigation of a Supersonic Scoop Inlet Derived From a Conical-Spike Nose Inlet. NACA RM L51G11, 1951.

[redacted]

12. Hasel, Lowell E.: The Performance of Conical Supersonic Scoop Inlets on Circular Fuselages. NACA RM L53I14a, 1953.

13. Valerino, Alfred S.: Performance Characteristics at Mach Numbers to 2.0 of Various Types of Side Inlets Mounted on Fuselage of Proposed Supersonic Airplane. I - Two-Dimensional Compression-Ramp Inlets With Semicircular Cowls. NACA RM E52E02, 1952.

14. Howell, Robert R., and Keith, Arvid L., Jr.: An Investigation at Transonic Speeds of the Aerodynamic Characteristics of an Air Inlet Installed in the Root of a 45° Sweptback Wing. NACA RM L52H08a, 1952.

[redacted]

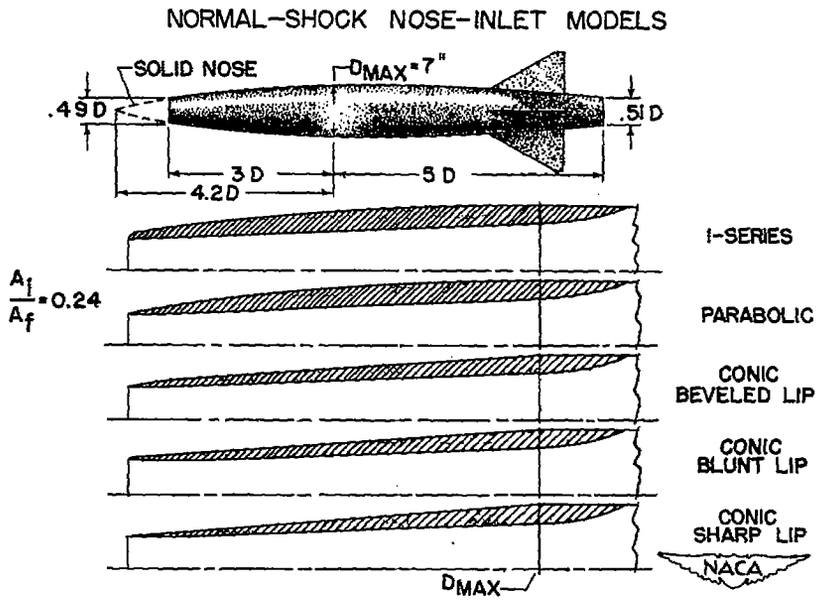

Figure 1

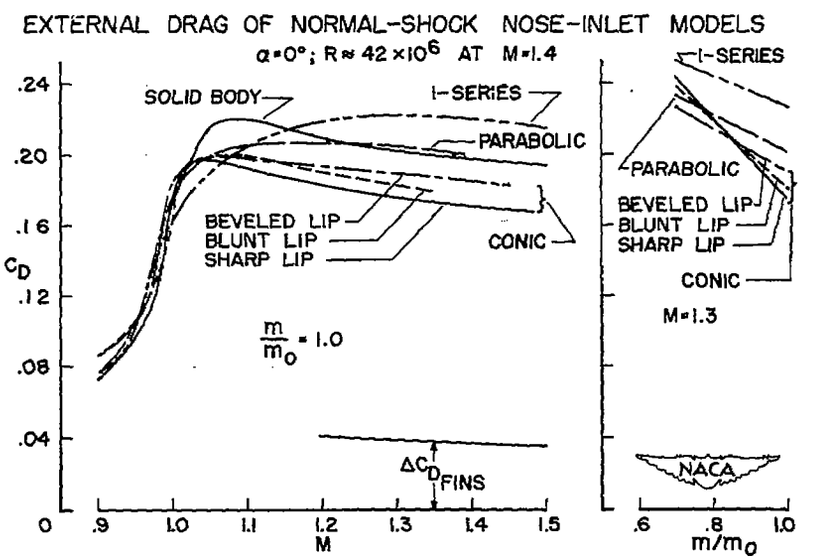

Figure 2

[redacted]

CONICAL-SHOCK INLET MODELS

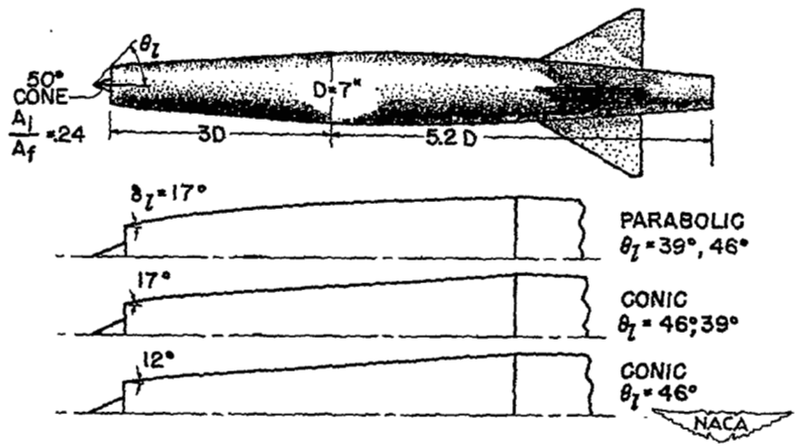

Figure 3

EXTERNAL DRAG OF CONICAL-SHOCK NOSE-INLET MODELS
α=0°; R≈42 x 10^6 AT M=1.4

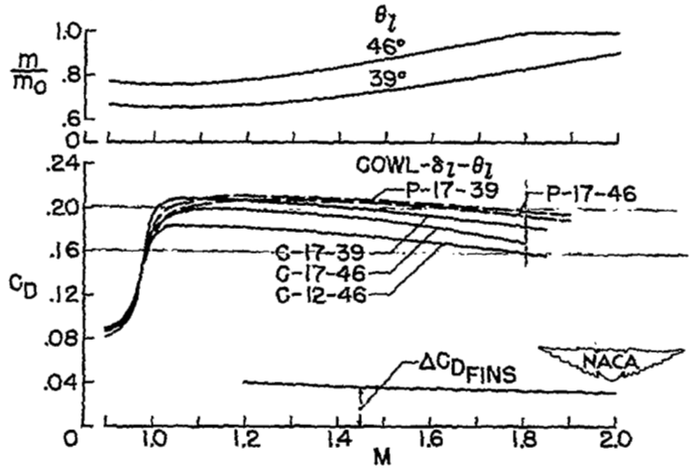

Figure 4

[redacted]

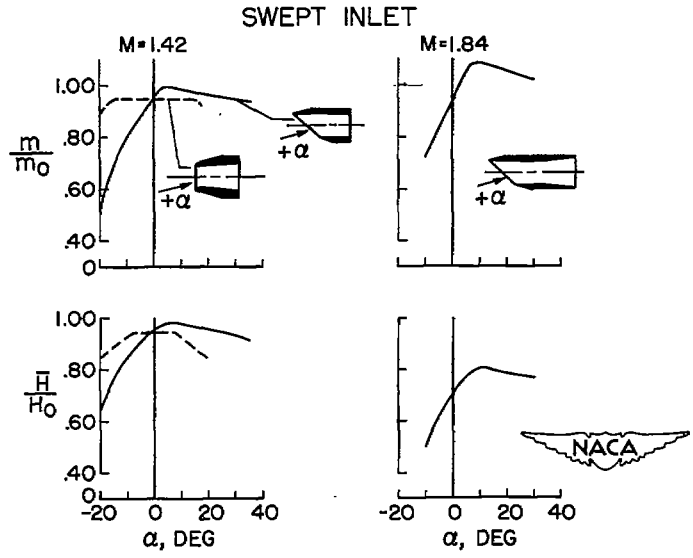

Figure 5

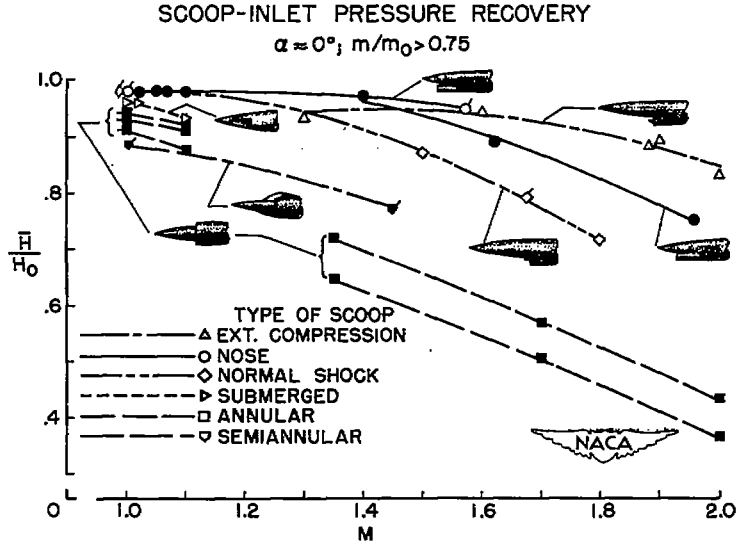

Figure 6

[redacted]

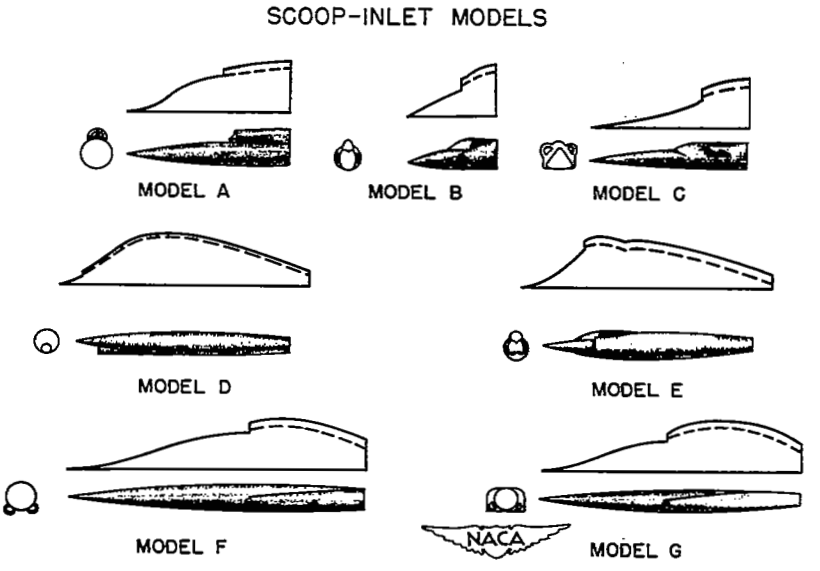

Figure 7

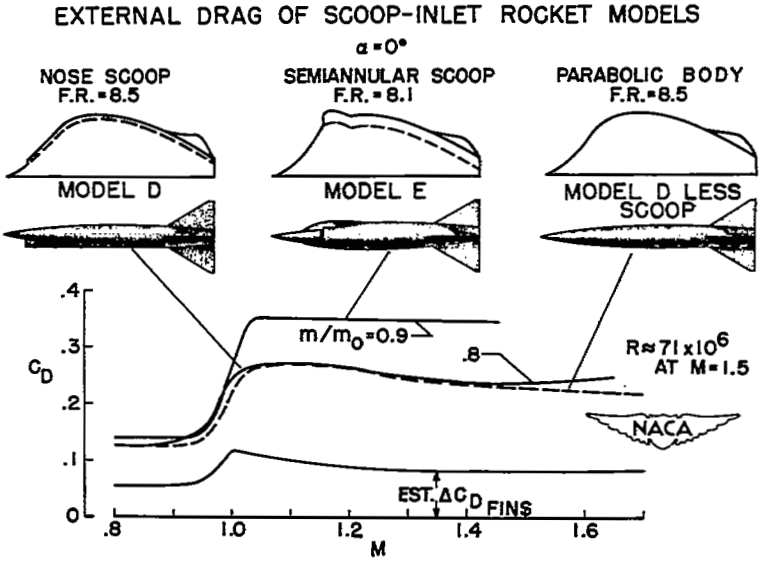

Figure 8

[redacted]

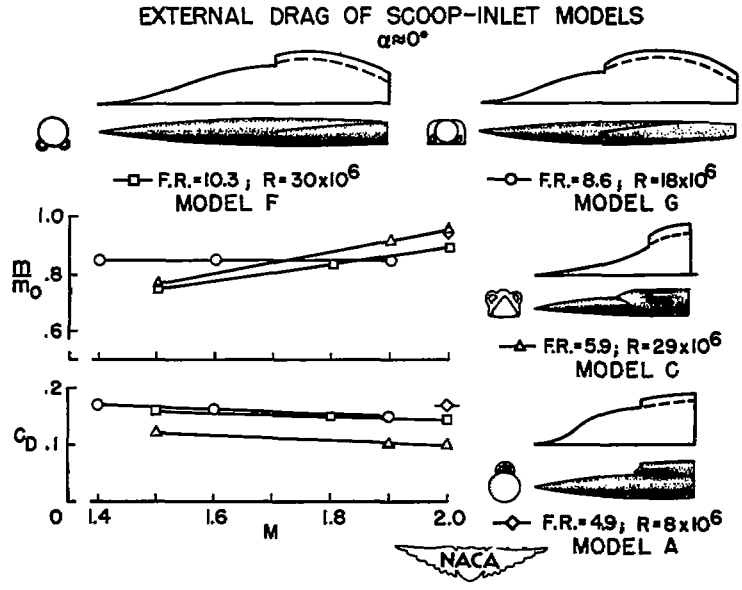

Figure 9

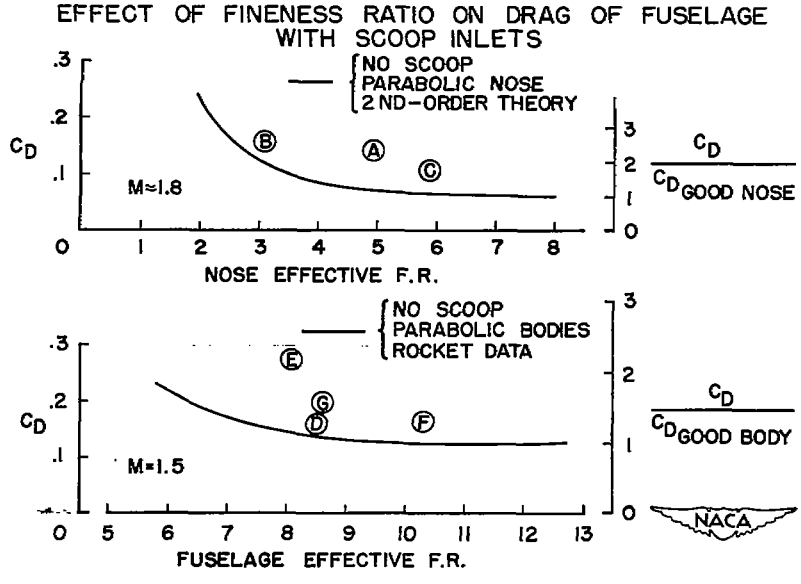

Figure 10

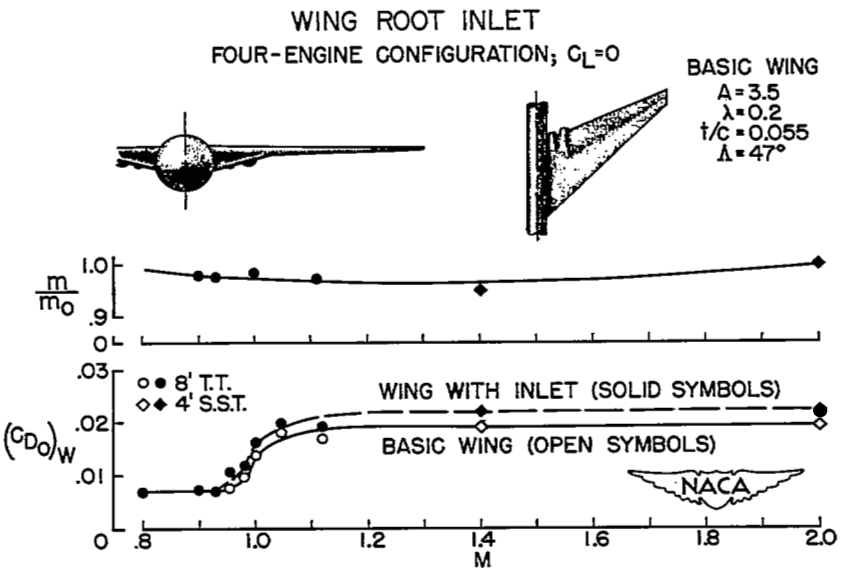

Figure 11

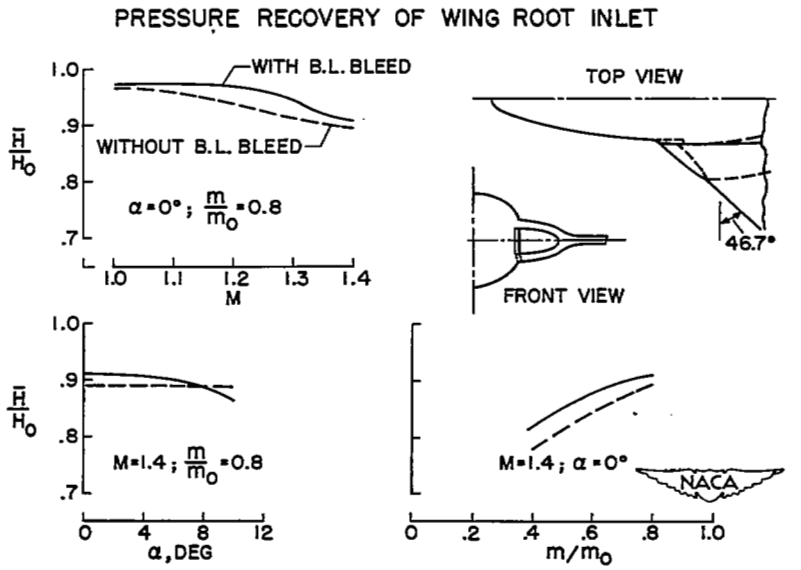

Figure 12